American Journal of Materials Science and Application
2015; 3(2): 38-43
Published online April 10, 2015 (http://www.openscienceonline.com/journal/ajmsa)

Properties of CrN Coating Prepared by Physical Vapour Deposition

P. M. Perillo

Micro and Nanotechnology, Atomic Energy National Commision, Buenos Aires, Argentina

Email address

perillo@cnea.gov.ar

To cite this article

P. M. Perillo. Properties of CrN Coating Prepared by Physical Vapour Deposition. *American Journal of Materials Science and Application*. Vol. 3, No. 2, 2015, pp. 38-43.

Abstract

The present study focused on growth of CrN coating deposited by plasma enhanced physical vapor deposition (PEPVD) on commercial titanium substrate. The composition, microstructure and residual stresses of the coatings were determined by scanning electron microscopy (SEM), photoelectron spectroscopy generated by X-rays (XPS / ESCA) and X-ray diffraction. To evaluate the performance against corrosion potentiodynamics polarization curves were performed in 0.1 N NaCl and H_2SO_4 5% solutions at room temperature and in nitrogen atmosphere. The results were compared with the uncoated material under the same experimental conditions. It was found that the coated materials have lower corrosion rate than the uncoated materials. The presence of the coating leads to an increase in resistance to polarization and a decrease of two orders of magnitude in the critical current density of passivation.

Keywords

Corrosion, Ti, PEPVD, CrN, Coating

1. Introduction

Chromium nitride coatings have been extensively used in industry as hard films to protect base materials because it have excellent properties like wear resistance, high hardness, good mechanical strenght, good adhesion, remarkable stability against oxidation and resist thermal heat treatment up to 600 °C among others [1,2]

Physical vapour deposition (PVD) and Chemical vapor deposition (CVD) techniques are the methods usually used to deposit chromium nitride films [3-6]. Whereas CVD methods are not as popular because all the available precursors are solid and are not efficient due to difficulty in handling and flow control.

The microstructure of the coatings produced by PVD is characterized by a columnar structure and local surface defects such as pores, defects [7,8] and eventually fractures. The corrosion resistance of the PVD coatings depends not only on the degree of porosity resulting mainly from the structural defects but also from factors, such as coating–substrate interface chemistry, structure, surface defect density , coating adhesion and residual stresses [9,10].

The corrosion problems observed in coating materials are generally the result of penetration of aggressive agents through these defects and their arrival at the substrate. The main obstacle is its susceptibility to crevice corrosion.

The addition of an intermediate metal layer has improved corrosion resistance because the columnar structure is blocked [11]. The use of multilayeres coatings would improve the corrosion resistance [12,13].

The present study investigates the properties (microstructure, hardness, residual stresses, adhesion) of CrN coatings deposited by PVD techniques on titanium substrates which would influence the corrosion behavior.

2. Experimental Procedure

2.1. Coating Deposition

Sheets of commercially pure grade titanium (99.8%) with dimensions of 15 mm x 10 mm x 0.5 mm thick were used as substrate. Prior to experiments, the titanium sheets were firstly smoothed and cleaned using sandpaper, then the foils were ultrasonically cleaned in isopropyl alcohol and acetone solution, afterwards rinsed with deionized water and finally

dried in a nitrogen stream.

The coatings were deposited by PEPVD in a R3-J RMP3 Nissin Electric equipment. After cleaning, the samples were inserted into the carrier substrate, the vacuum chamber was evacuated to approximately 6.6 x 10^{-3} Pa. The temperature was controlled by a chromel alumel thermocouple. The coatings were deposited with a cathode arc current of 80 A with a negative substrate bias of 300 V and a substrate current of 1 A. Cathode was used as pure chromium (99.8%). A mixture of argon and nitrogen in ratio 1:30 was used and the total pressure in the chamber was 3.99 Pa. The CrN coating include a thin pre-deposited (< 200 nm) metallic Cr interlayer. After 15 minutes the temperature was raised to 300 °C and then remained constant. The thickness of the coatings was controlled by deposition time and was adjusted to generate a thickness of ~3 μm.

2.2. Characterization of CrN Coating

The samples were characterized by scanning electron microscopy (SEM), X-ray diffraction (XRD) and X-ray photoelectron spectroscopy (XPS). Scanning electron microscope (Fei model Quanta 200) was employed for the morphological charactherization of the CrN coatings. The thickness of the coating was measured using the Calotest method [14].

X-ray diffraction (XRD) patterns were recorded at room temperature with Cu Kα radiation of 0.15418 nm in a diffractometer (Philips X'Pert) using conventional Bragg-Brentano (BB) diffraction geometry. The data were collected for scattering angles (2θ) ranging from 30° to 85° with a step 2θ of 0.02° for 1 s by step. The composition of phases, residual stresses and crystallographic texture of the CrN coatings, were characterized by X-ray diffraction.

The coating chemical elements and their bonding condition were characterized using X-ray photoelectron spectroscopy (XPS) (Vacuum Generator Mod. ESCA 3 MARK II) The X-ray in XPS was generated at 10 kV and 20 mA, using Mg Kα radiation (hv =1253.6 eV). The air pressure in the vacuum chamber was 7×10^{-9} Torr. The depth profile analyses of the near surface regions were carried out by sputtering with Ar+ ions using a current intensity of 6 μA and an acceleration voltage of 5 kV (ion current, 8 μA) at an argon pressure of 8×10^{-5}mTorr. All the experiments were conducted at room temperature. Spectra of Si 2p, O 1s and C 1s were recorded to measure concentration profiles.

The Vickers hardness of the CrN coated substrate was measured using an Akashi MVK-H2 microhardness tester.

In order to prevent from substrate effect a load of 25 gf was applied to the sample [15].

A LSRH-REVETEST scratch tester was used to determine the adhesion characteristics.The scratch tests were performed under the standard conditions (diamond stylus R = 0.2 mm; scratching speed 10 mm/min; loading rate 100 N/min). In the scratch experiments, we measured the scratch channel width and from this value calculated the scratch depth 6 from trigonometry as a function of the applied load considering a spherical indenter with a measured radius of 200 pm.

2.3. Electrochemical Measurements

Corrosion resistance was investigated by potentiodynamics polarization curves with coated and uncoated probes in 5% H_2SO_4 and NaCl 0.1 N solution in nitrogen atmosphere, at room temperature, in conventional corrosion cells. Electrochemical measures were obtained using a Gamry PC4/750 potentiostat/galvanostat. The electrode potential was measured through a Luggin capillary. A saturated calomel electrode (SCE) or sulfate electrode (SE) and a platinum wire (surrounding the specimen) were employed as the reference electrode and the counter electrode, respectively. Before all electrochemical measurements, specimens were held immersed in the solution to reach a stationary corrosion potential for 60 min before testing. To avoid crevice corrosion a protective acetate lacquer was used to mask the samples, allowing 1 cm^2 of their surface to be in contact with the solution. The polarization curves of all the specimens were generated after conducting the scan from −200 mV below corrosion potential at a scan rate of 0.167 mV/s. The solutions were prepared from analytical grade materials and distilled water.

3. Results and Discussion

3.1. Crystalline Phases

Figure 1 shows the phases present in the coating and the substrate.

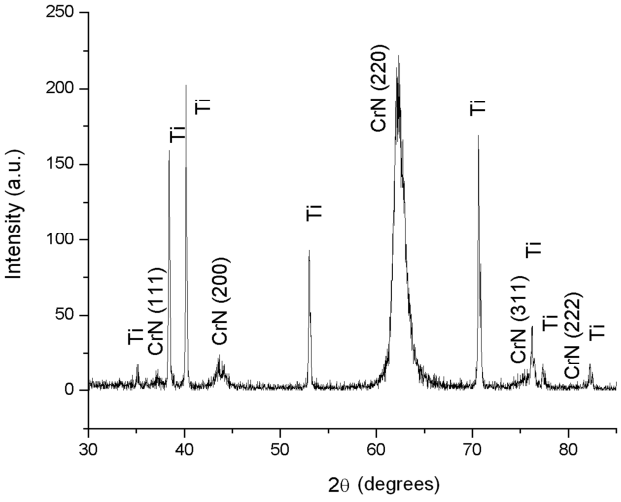

Figure 1. *XRD patterns of Cr/CrN coating on Ti.*

It is observed that the cubic phase (FCC) of CrN (NaCl type crystal structure) is predominant in the coating and low proportion of low intensity peaks corresponding to the interlayer of Cr are detected. The substrate has the Tiα hcp crystalline structure phase.

In Table 1 are shown the diffraction peaks for the coating of CrN corresponding to planes (111), (200) and (220), also indicating the values of lattice parameters ahkl and the peak widths (FWHM) [16].

Table 1. *Parameters obtained from XRD-BB diagrams for CrN coating. Tabulated value ao (CrN)= 4.148Å for a stress-free standard pattern.*

CrN (hkl)	CrN $2\theta_{hkl}$ (°)	CrN a_{hkl} (Å)	CrN FWHM (°)
(111)	37.20	4.1829	0.442
(200)	43.63	4.1485	0.647
(220)	62.30	4.2115	0.973

From Table 1 it is observed that the lattice parameters of CrN are greater than the tabulated values (JCPDS card 11-0065) and the peak positions are shifted to lower values than those tabulated, it indicates the presence of compressive residual stresses in the coating due to the applied bias voltage.

3.2. Crystallographic Texture Pole - Figures

The characterization of preferential orientations of the CrN coating and Ti substrate was performed from measurements of pole figures (PF).

The diffracted intensity distribution of planes of CrN (111) (200) and (220) for different rotations was determined: ψ angles between the surface normal to the sample and the surface normal to the plane (hkl) and ϕ rotation angles about surface normal to the sample. The distribution of intensities measured at different positions (ψ, ϕ) of the sample for a fixed position of the angle 2 θ diffraction (Table 1) is displayed in a stereographic projection in the form of pole figures (PF) for each reflection (HKL). For ψ (0^o- 80^o) = 5^o and ϕ (0^o-360^o) = 1 s time by step were chosen.

The measurements of PF in Ti substrate were made to the crystalline planes (0002), (10 $\bar{1}$0) (11 $\bar{2}$0) under the same experimental conditions as the coating.

The texture main component of the Ti substrate represents the majority of the crystals parallel to the {0002} sample surface planes.

In Figure 2 the PF (111), (200) and (220) of the CrN coating on Ti substrate are shown.

The main peaks are located around the center of the PF (220) and correspond to the texture reinforcement with crystals oriented parallel to the normal direction (ND) to the sample crystal planes (220).

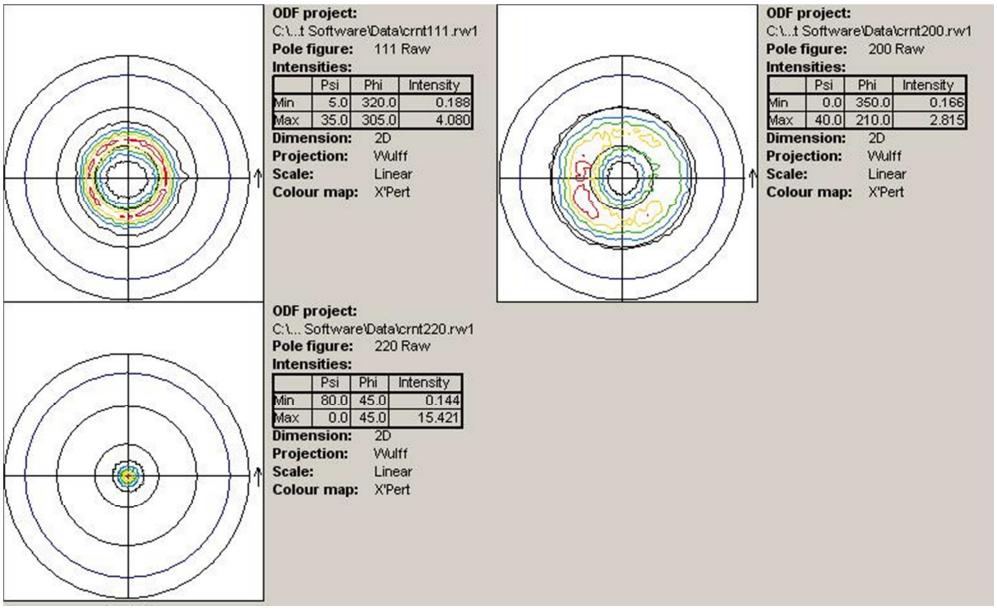

Figure 2. *PF (hkl) of CrN coating deposited on Ti.*

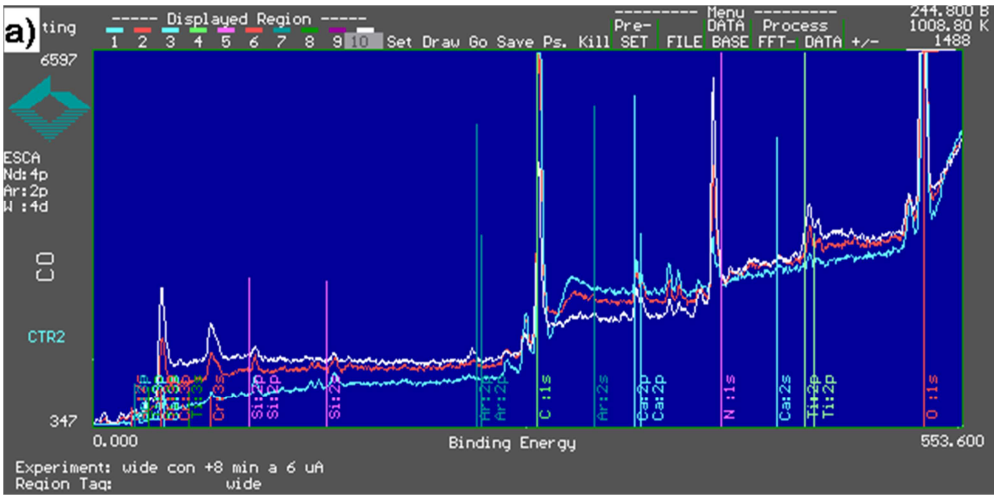

Figure 3. *Wide spectrum of Cr a) before and b) after scanning with Ar^+ ions*

3.3. Residual Stresses

Table 2 shows the values of residual stresses (σ) and values of diffraction peak width (FWHM) as indicative of the level of microdeformations.

Table 2. *Values of residual stresses, peak width and crystallographic texture CrN coating and Ti substrate.*

Material	σ (GPa)	FWHM (°)	Texture
Substrate Ti	-0.11±0.01	0.318	(0002) I_{max}: 6.11
Coating CrN	-3.47±0.40	1.367	(220) I_{max}: 15.42

The compressive residual stresses and microstrains in the CrN coating are very high compared to the Ti substrate, due of the deposition process that produces a strong expansion of the crystal lattice of CrN [17,18].

3.4. Chemical Characterization

The XPS investigations of the surface of the film show the presence of the elements Cr and N [19]. The samples showed a significant surface contamination of C, O and Si. The C and O were virtually eliminated with a cleaning sweep during 8 minutes with Ar^+ ions. Narrow spectrum of Cr is shown in Figure 3. The peak deconvolution was made for different groups of chemical species Cr^0 (574,3±0,4 eV), N linked Cr (CrN, Cr_2N, CrN_xO_y (575,7±0,4 eV), Cr^{III} with O (Cr_2O_3, $Cr(OH)_3$; CrO(OH)) (576,8±0,4 eV).

The narrow spectrum of CrN shown in Figure 4. The deconvoluted peak was taken for different groups of chemical species. Cr^0 (574.3 ± 0.4 eV), N-linked Cr (CrN, Cr_2N, CrN_xO_y (575.7 ± 0.4 eV), Cr^{III} with O (Cr_2O_3, Cr $(OH)_3$, CrO (OH)) (576.8 ± 0.4 eV).

3.5. SEM Morphology

Cross section image of the CrN coating is shown in Fig 5 a. The CrN coating deposited at high bias voltage (–300 V) was composed of a fine-grained, dense non columnar microstructure [20]. The high substrate bias voltage also induces energetic particle bombardment during the film deposition with the appearence of droplets and the increasing the surface roughness (Fig 5b). The fine-grained CrN coating can be expected to perform better in an aggressive aqueous environment.

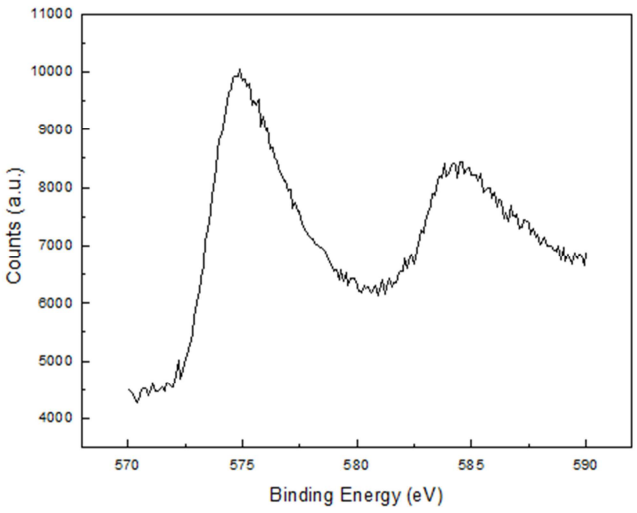

spectrum core Remove that paragraph

Figure 4. *Narrow spectrum of CrN*

3.6. Adhesion

CrN have two types of failure by observation with low magnification optical microscopy [21].

As shown in Fig 6. depicting a typical result from a scratch test, the very initial crack generation point during scratch testing was taken as the first critical load (LC1: 18,8 N). Lateral faults that arise over the groove striped considered cohesive failure and the point of complete delamination was taken as the adhesion failure critical load (LC2: 33,5 N). No coating was observed in the center of the groove are considered adhesive failure.

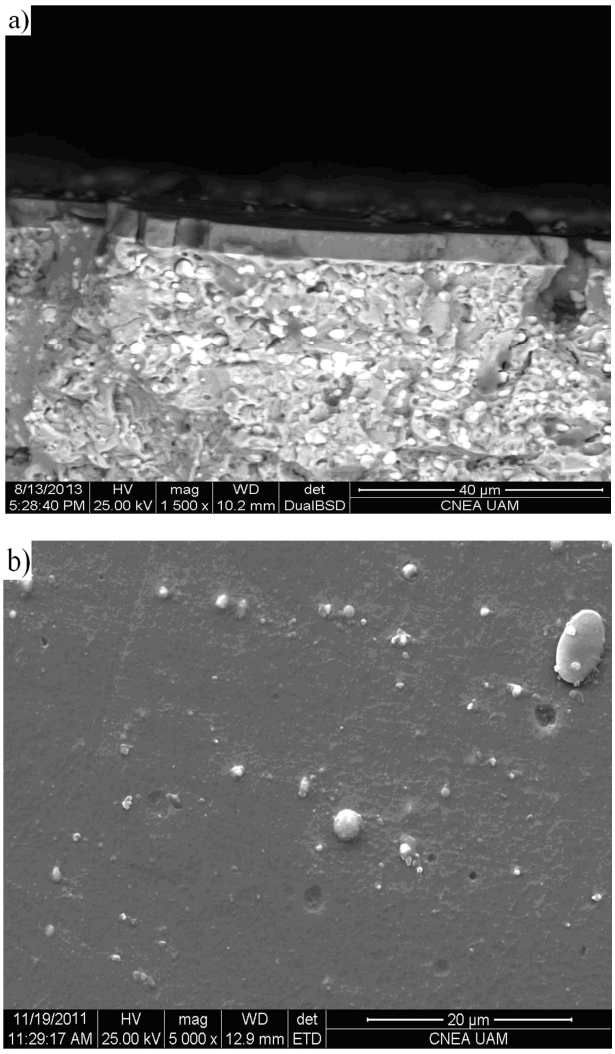

Figure 5. *SEM micrographs of CrN a) cross sectional b) top view.*

3.7. Electrochemical Tests

The corrosion resistance was determined by plotting the anodic potentiodynamics polarization curves of coated and uncoated specimens with a scan rate of 0.167 mV/s. Media tested were 0.1 M NaCl and 5% H_2SO_4 solution, prepared with analytical grade reagents and distilled water. All experiments were performed in de-aerated solutions with high purity N_2 at room temperature. Conventional three electrode corrosion cells were used with a Pt wire as counter electrode surrounding the specimen. The electrode potential was measured through a Luggin capillary, using a saturated calomel reference electrode (SCE) and a Silver/Silver sulfate reference electrode. All potential values are expressed in the normal hydrogen scale (NHE).

To prevent corrosion cracks a lacquer acetate was used for the samples, leaving an area of 1 cm^2 in contact with the solution. The test pieces were immersed in the liquid for 1 hour prior to the test, to reach a stable corrosion potential.

Fig. 7 shows the anodic polarization curves in 0.1M NaCl solution for uncoated and coated titanium. The bare substrate has a nearly constant current density of the order of 10^{-6} A/cm^2 up to potential values close to 1.5 V, due to the presence of a passivating film of TiO_2. Then, the current density shows a marked increase, but for higher potentials, in the range between 2 and 3 V, again remains constant at a value of the order of 10^{-6} A/cm^2.

The coated sample has a more positive corrosion potential (E corr) value. The current density gradually increases to a potential value close to 1.25 V. From that potential the current density decreases to 10^{-3} A/cm^2, probably due to the formation of a passivating film of TiO_2.

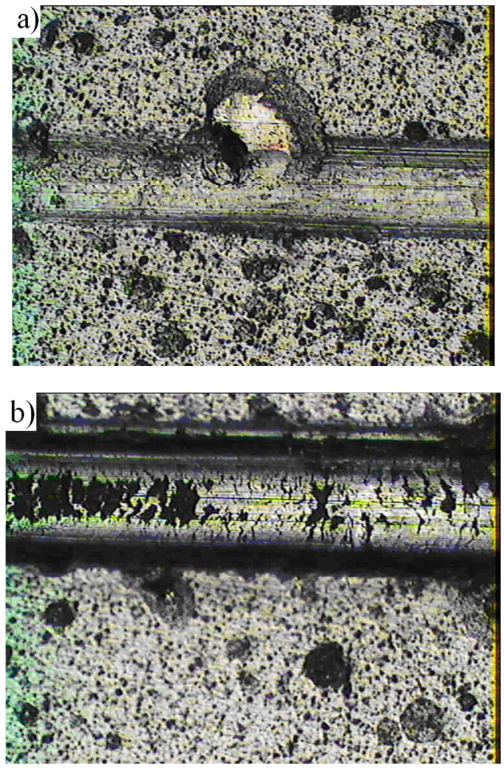

Figure 6. *Optical microscope photographs of failure modes a) cohesive b) adhesive mode for CrN coatings on Ti.*

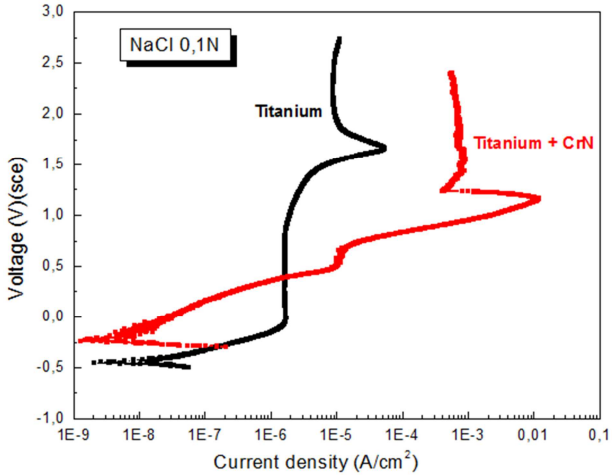

Figure 7. *Polarization curve of Ti and Ti coated with CrN in 0.1 M NaCl solution.*

Fig.8 shows the comparison between the polarization curves for coated and uncoated Ti substrates in 5% H_2SO_4 solution. A significant change in the corrosion potential E_{corr}

between the coated and uncoated substrate. This means that the coating shifts the corrosion potential to more positive potential values and consequently protects from corrosion to a different extent.

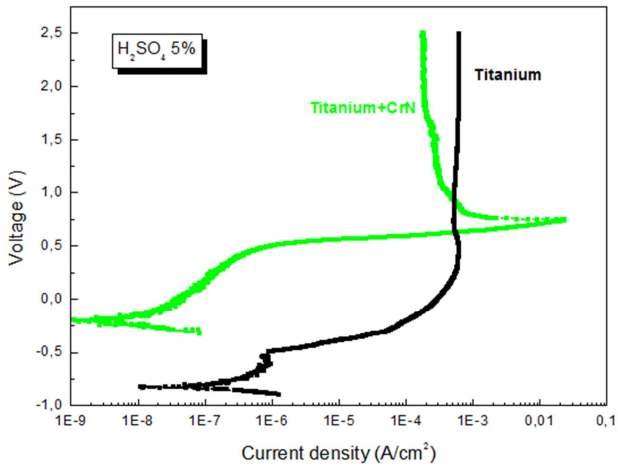

Figure 8. *Polarization curve of Ti and Ti coated with CrN 5% H_2SO_4 solution.*

4. Conclusions

The CrN coatings with the dense structure and fine equiaxed crystallites makes them less permeable to the corrosive medium. A lack of straight diffusion channels because of the non-columnar structure whereby the oxygen diffusion rate is significantly reduced.

Although single-layer coating reduce the overall dissolution rate, the corrosion process of the coated titanium is still dominated by relatively rapid local dissolution of the substrate at through-coating pinholes.

The improvement of the corrosion resistance by CrN coatings is two orders of magnitude in the critical current density of passivation.

References

[1] C.M. Suh, B.W. Hwang, R.I. Murakami Behaviors of residual stress and high-temperature fatigue life in ceramic coatings produced by PVD Mat. Sci. Eng A 343 (2003) 1–7.

[2] F.R. Lamastra, F. Leonardi, R. Montanari, F. Casadei, T. Valente, G. Gusmano, X-ray residual stress analysis on CrN/Cr/CrN multilayer PVD coatings deposited on different steel substrates Surf. Coat. Techn. 200 (2006) 6172-6175.

[3] V. Ezirmik, E. Senel, K. Kazmanli, A. Erdemir b, M. Ürgen, Effect of copper addition on the temperature dependent reciprocating wear behaviour of CrN coatings Surf.Coat. Techn. 202 (2007) 866-870.

[4] B. Warcholinski, A. Gilewicz, Z. Kuklinski, P. Myslinski Hard CrCN/CrN multilayer coatings for tribological applications Surf Coat. Techn. 204 (2004) 2289-2293.

[5] N.E. Beliardouh, K. Bouzid, C. Nouveau, B. Tlili, M.J. Walock Tribological and electrochemical performances of Cr/CrN and Cr/CrN/CrAlN multilayer coatings deposited by RF magnetron sputtering Tribology Intern. 82 (2015) 443-452.

[6] P.Eh. Hovsepian, D.B. Lewis, Q. Luo,T, A. Farinotti Corrosion resistance of CrN/NbN superlattice coatings grown by various physical vapour deposition techniques, Thin solid films 488 (2005) 1-8.

[7] L. Cunha , M. Andritschky, Residual stress, surface defects and corrosion resistance of CrN hard coatings Surf. Coat. Techn. 111 (1999) 158–162.

[8] C. Petrogalli, L. Montesano, M. Gelfi, G.M. La Vecchia, L. Solazzi Tribological and corrosion behavior of CrN coatings: Roles of substrate and deposition defects Surf Coat. Techn. 200 (2014) 878-885.

[9] M. Tomlinson,S.B. Lyon,P. Hovsepian,W-D. Munz Corrosion performance of CrN/NbN superlattice coatings deposited by the combined cathodic arc/unbalanced magnetron technique Vacuum Vol 53, Issues 1–2, (1999) 117–121.

[10] Ruden, E. Restrepo-Parra, A.U. Paladines, F. Sequeda, Corrosion resistance of CrN thin films produced by dc magnetron sputtering Applied Surf. Sci. 270 (2013) 150-156.

[11] S.Han, J.H.Lin. X.J.Guo, S.H.Tsai, Y.O.Su, J.H. Huang, F.H.Lu, H.C.Shih The effect of Cr interlayer on the microstructure of CrN coatings on steel Thin Solid Films 377-378 (2000) 578-584.

[12] Y.L. Chipatecua, J.J. Olaya, Diego F. Arias, Corrosion behaviour of CrN/Cr multilayers on stainless steel deposited by unbalanced magnetron sputtering, Vacuum 86 (2012) 1393-1491.

[13] C. Liu, A. Leyland, Q. Bi, A. Matthews, Corrosion resistance of multi-layered plasma-assisted physical vapour deposition TiN and CrN coatings, Surf. and Coat. Techn. 141 june 2001 pp 164-173.

[14] H. Pulker, “Wear and Corrosion Resistance Coatings by CVD and PVD” E. Horwood, Halsted Press (Chichester, New York) 1989.

[15] Rodrigo, P. Perillo, H. Ichimura On the correlation of substrate microhardness with the critical load of scratch adherence for hard coatings Surf. Coat.Techn. 124 (2000) 87–92.

[16] Barata, L. Cunha, C. Moura Characterisation of chromium nitride films produced by PVD techniques Thin Solid Films 398–399 (2001) 501–506.

[17] F.R. Lamastra, F. Leonardi, R. Montanari, F. Casadei, T. Valente, G. Gusmano X-ray residual stress analysis on CrN/Cr/CrN multilayer PVD coatings deposited on different steel substrates, Surf Coat. Techn. 200 (2006) 6172-6175.

[18] Ch.M. Suh , B.W. Hwang, R.I. Murakami, Behaviors of residual stress and high-temperature fatigue life in ceramic coatings produced by PVD, Mat Sci. Eng A 343 (2003) 1-7.

[19] Lippitz, Th.Hübert. “XPS investigations of chromium nitride thin films” Surf. Coat. Techn. 200 (2005) 250-253.

[20] Warcholinski, A. Gilewicz Effect of substrate bias voltage on the properties of CrCN and CrN coatings deposited by cathodic arc evaporation, Vacuum 90 (2013) 145-150.

[21] M. Nordin, M. Larsson, S. Hogmark Mechanical and tribological properties of multilayered PVD TiN/CrN Wear 232 (1999) 221-225.